Journal of Statistical Physics, Vol. 89, Nos. 3/4, 1997

Relaxation Time for a Dimer Covering with Height Representation

Christopher L. Henley[1]

Received August 6, 1996; final May 15, 1997

This paper considers the Monte Carlo dynamics of random dimer coverings of the square lattice, which can be mapped to a rough interface model. Two kinds of slow modes are identified, associated respectively with long-wavelength fluctuations of the interface height, and with slow drift (in time) of the system-wide mean height. Within a continuum theory, the longest relaxation time for either kind of mode scales as the system size N. For the real, discrete model, an exact *lower* bound of $O(N)$ is placed on the relaxation time, using variational eigenfunctions corresponding to the two kinds of continuum modes.

KEY WORDS: Dimer packing; height model; dynamic critical phenomena; solid-on-solid models; frustrated Ising models; quantum spin models; Markov chain algorithm.

1. INTRODUCTION

Statistical models in which each microstate maps to an interface—which I will call "height models"—tend to be interesting, for the interface is often rough, and it turns out the model has critical correlations.[1-8] This paper considers the corresponding *dynamics*, using one of the simplest lattice statistical models: the dimer covering of the square lattice.[9, 10] The dimers are placed on the bonds and every site must be touched by exactly one dimer. (This is equivalent, of course, to the packings of "dominoes" of size 2×1;[11] furthermore the ground states of the fully frustrated Ising model on the square lattice[12] map 2-to-1 to the dimer coverings.) In this paper,

[1] Department of Physics, Cornell University, Ithaca, New York, 14853-2501.

0022-4715/97/1100-0483$12.50/0

I only consider the case where each packing has equal weight. The system is taken to be a square of $L \times L$ sites with periodic boundary conditions for the dimers.

The statics can be described by mappings to free fermions, and exact solutions are possible using Pfaffians[9, 10] or transfer matrices.[13, 14] There is a nonzero ground state entropy of 0.2916 per site.[9] The correlation functions are critical[15] (power-law decaying). This is easiest understood after mapping the dimer packings (configuration-by-configuration) to configurations of "heights" $z(\mathbf{r})$ living on dual lattice sites, $\mathbf{r} = (x, y)$, representing a rough interface in an 3-dimensional abstract space.[1-8]

When such a model is endowed with dynamics, a central question is how the equilibration time $\tau(L)$ (to be defined shortly) scales as a function of the system diameter L. In particular, what is the dynamic exponent z[16] in $\tau(L) \sim L^z$? Since the static continuum model has a gradient-squared free energy, one would suspect that $z = 2$. Indeed, scaling with $z = 2$ has been seen numerically in simulations of the square lattice dimer model.[18] (It has also been seen in antiferromagnetic Ising models[7] and random-tiling quasicrystal models[19] with height representations.) However, it has only been proven[20] that (with our definition of time scale) $\tau(L) \leqslant O(N^3)$, which implies $z \leqslant 6$.

This paper has two aims: (i) an explicit approximate description of the slowest eigenmodes of the time evolution, based on continuum theory—this theory is applicable, with small changes, to any height model; (ii) the outline of a proof that $\tau(L) \geqslant O(L^2)$ (and hence $z \geqslant 2$).

The outline of the paper is as follows. The remainder of this section specifies the model, in particular the height mapping and dimer-flip stochastic dynamics, and also points out an exact correspondence of the *entire spectrum* of the quantum dimer model to that of this dynamics. I then take up a continuum model in terms of the height representation (Sect. 2) which is defined by standard Langevin dynamics, verifying that this is the appropriate coarse-graining of the microscopics. This produces an approximate description of *all* the slow eigenmodes (Sect. 2 and 3). Intriguingly, the slowest mode in any finite-size system is *not* the longest-wavelength capillary wave, but a "height-shift" mode involving diffusion of the system-wide average "height" direction (Sect. 3).

Finally (in Sect. 5) I explain how rigorous bounds on the dynamics can be proven. The fundamental concepts for this proof are (i) the use of Fourier analysis to partially diagonalize the evolution matrix $\mathscr{W}$, (ii) constructing variational "wavefunctions" guided by the results of the earlier sections, and (iii) taking advantage of the Fourier spectrum of height fluctuations derivable from the exact solution of the model. In the conclusion, I mention other spin models to which these results should be relevant.

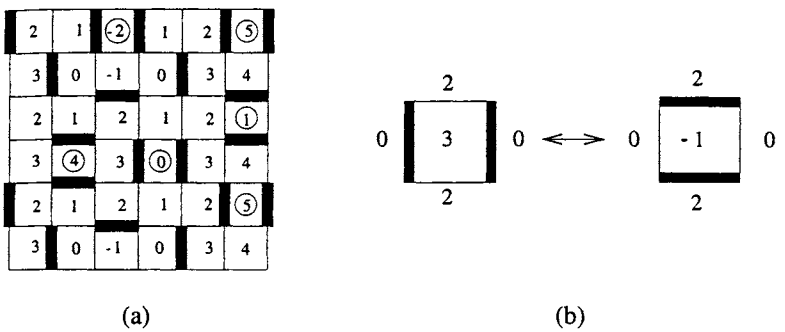

Fig. 1. (a). Random dimer packing, showing heights $z(\mathbf{r})$ (those in flippable plaquettes are circled). (b). Elementary dimer flip, showing heights.

A. Height Representation

The explicit rule for constructing a height pattern $\{z(\mathbf{r})\}$, given a snapshot of the dimers, is shown in Fig. 1: $z(\mathbf{r}) - z(\mathbf{r}') = -3$ if there is a dimer between $\mathbf{r}$ and $\mathbf{r}'$, or $+1$ if there is no dimer, where the step from $\mathbf{r}$ to $\mathbf{r}'$ is taken in a counterclockwise sense about the even sites. The net height difference is zero for the path around one plaquette, and hence by induction for any closed path, showing the consistency of the definition. However, it is nonunique in that adding the same constant to each $z(\mathbf{r})$ makes an equally valid height representation of the same dimer configuration; I shall fix this constant after defining the dynamics (below).

It is necessary in writing the continuum model for $z(\mathbf{r})$ (e.g., to define its Fourier transform) that $z(\mathbf{r})$ satisfy periodic boundary conditions; but periodic boundary conditions for dimers only imply $z(L, y) - z(0, y) = w_x$ and $z(x, L) - z(x, 0) = w_y$, where the "winding numbers" w_x and w_y are multiples of 4, so that the system has a mean tilt is $(w_x/L, w_y/L)$. *Local* update rules (such as I am about to define) conserve the winding numbers. Thus one could define substracted heights $z'(x, y) \equiv z(x, y) - (w_x/L)\, x - (w_y/L)\, y$ which do satisfy periodic boundary conditions. In the limit of small tilts, $z'(\mathbf{r})$ would obey the same continuum dynamics.[2] This trivial generalization is not worth the added complication in notation; in the remaining sections I will consider only configurations with $(w_x, w_y) = (0, 0)$.

The ground states of the fully-frustrated Ising model on the square lattice may be mapped (2-to-1) to dimer coverings of the dual square lattice. The rule is: simply draw a dimer across every violated bond. Therefore that

[2] If tilts are nonvanishing as $L \to \infty$, the free-energy functional (7) must be generalized to have different stiffnesses for components of the gradient parallel to and transverse to the tilt direction; the same power laws for the dynamics would be deduced.

model has a height representation and all my results apply equally to the fully-frustrated Ising model.

The height variable will play the role of the "order parameter" in this paper. The more customary order parameter, for *any* of the height models, is a spin operator $m(\mathbf{r})$ (or a dimer occupation operator, in the present case). However, as outlined in Appendix A, such an $m(\mathbf{r})$ is simply a sinusoidal function of the local height. Since the long-distance and longtime height fluctuations discussed here are Gaussian, it is possible from them to compute the correlations of $m(\mathbf{r})$ which turn out to be algebraic with non-universal exponents.

B. Dynamics

It is possible to turn any dimer covering (of zero mean tilt) into any other one by a succession of "dimer flips" each affecting two dimers on opposite edges of one plaquette (see Fig. 1b). Thus the model is endowed with a stochastic (Monte Carlo) dynamics in continuous time as follows: select plaquettes at random, at a rate N per unit time where $N \equiv L^2$ is the number of sites (i.e., on average visit each plaquette once per unit time). Flip the plaquette if it has two dimers as in Fig. 1b, otherwise do nothing.

On the other hand, the natural zero-temperature dynamics of the fully frustrated Ising model is to choose a spin at random and flip it if the energy change would be zero, otherwise do nothing. This induces exactly the same dynamics on the dimer configurations as specified in the preceding paragraph.

To eliminate the arbitrariness in defining $z(\mathbf{r})$ and ensure that the coarse-grained dynamics is continuous in time, we relate $z(\mathbf{r}, t)$ at different times, by specifying that a dimer flip on a plaquette changes only the $z(\mathbf{r})$ value in that plaquette's center. (Notice that the possible $z(\mathbf{r})$ values on a particular site can only differ from the initial value by a multiple of 4; the values of $z(\mathbf{r})$ (mod 4) define four fixed, square sublattices.[2])

Now let $\{p_\alpha(t)\}$ be the probability of being in microstate α at time t. The master equation states

$$\frac{dp_\alpha(t)}{dt} = \sum_{\langle \alpha \to \beta \rangle} (p_\beta - p_\alpha) \equiv -\sum_\beta \mathscr{W}_{\alpha\beta} p_\beta \tag{1}$$

where $\langle \alpha \to \beta \rangle$ means summing over configurations β which differ from α by one dimer flip; thus

$$\mathscr{W}_{\alpha\beta} = F_\alpha \delta_{\alpha\beta} - \mathscr{A}_{\alpha\beta} \tag{2}$$

where $\mathscr{A}$ is the adjacency matrix (elements unity if α and β are related by a flip, and zero otherwise), and $F_\alpha \equiv \sum_\beta \mathscr{A}_{\alpha\beta}$ is the number of "flippable" plaquettes in configuration α. These matrices are $M_0 \times M_0$, where M_0 is the number of microstates. It is well known that the matrix $\mathscr{W}$ has nonnegative eigenvalues (via the Perron–Frobenius theorem, since $\mathscr{W}$ is a stochastic matrix). The eigenvector of zero eigenvalue is $p_\alpha = 1/M_0$, the weight of the (equilibrium) steady state (which is unique, since dimer flips connect all microstates). Furthermore, any time correlation function in the system can be resolved into a sum over eigenvalues λ of $\mathscr{W}$, in the form

$$\sum_\lambda c_\lambda e^{-\lambda t} \tag{3}$$

Then it is normal to define the system's equilibration time

$$\tau(L) = \lambda'^{-1}_{\min} \tag{4}$$

where $\lambda'_{\min}$ is the smallest nonzero relaxation rate, the inverse of the second smallest eigenvalue of $\mathscr{W}$.

C. Quantum Dimer Model

In the quantum dimer model, the basis states are taken to be the dimer coverings, and the Hamiltonian is taken to have matrix elements

$$\mathscr{H}_{\alpha\beta} = -\mathscr{A}_{\alpha\beta} + VF_\alpha \delta_{\alpha\beta} \tag{5}$$

The first term describes dimer flips—like a particle quantum "hopping" with amplitude unity on the microstate graph; the second term is a "potential energy" which penalizes each flippable plaquette.

When $V = 1$, obviously

$$\mathscr{H}_{\alpha\beta} = \mathscr{W}_{\alpha\beta} \tag{6}$$

Ref. 21 noted that (6) implies the ground state wavefunction of (5) is a superposition of all the dimer packings with equal amplitudes. In other words, that (quantum) wavefunction is proportional to the steady-state probabilities of the (classical) dynamics (1).

Here I note that (6) further implies a one-to-one correspondence of *all* the eigenstates of (5) to normal modes of the master equation. Thus the bounds derived in this paper for the slowest relaxation rate are equally valid for the energy gap in the quantum model, and the approximate

eigenfunctions and eigenvalues found in Sect. 2 and 3 also describe the low-energy spectrum of the quantum dimer model.

2. CONTINUUM THEORY OF DYNAMICS

This section develops the continuum ("coarse-grained") version of the dynamics. In this form the model has an easily visualized physical meaning and (being linear) is solvable by standard and almost trivial techniques. In general, the slowest modes are associated with relaxation of the "order parameter";[16, 22] in the dimer covering model, the height variable plays the role of a (hidden) order parameter, so the dynamics are phrased in terms of it.

It should be noted that this theory is general to all rough height models.[3] The only specific information from the dimer model is the numerical value of the elastic constant K and of the height space lattice constant a_h, which are also known for many other height models.

A. Continuum Equations and Fourier Modes

First I review the coarse-grained picture of the height dynamics. The static free energy functional has the form

$$F = \int_{[0,\, L]^2} d^2\mathbf{r}\, \frac{K}{2} |\nabla h(\mathbf{r})|^2 \tag{7}$$

Here $h(\mathbf{r})$ represents a smoothed version of $z(\mathbf{r})$ and K is the stiffness constant controlling the fluctuations of the "interface." (From here on I assume zero net tilt of $z(\mathbf{r})$ and of $h(\mathbf{r})$ so these variables satisfy periodic boundary conditions.) The fact that the dimer model is rough (described by (7)) is nontrivial: several other height models, defined in similar ways, are found[5–8] in which the interface turns out to be smooth, or marginal. The roughness is confirmed only through the calculation in Appendix B.

The customary dynamics for such a field theory (see, e.g., ref. 22) is formulated as a Langevin equation,

$$\frac{dh(\mathbf{r})}{dt} = -\Gamma \frac{\delta F(\{h(\cdot)\})}{\delta h(\mathbf{r})} + \zeta(\mathbf{r}, t) \tag{8}$$

Here Γ is the kinetic (damping) constant measuring the linear-response to the force $\delta F/\delta h(\mathbf{r})$, and $\zeta(\mathbf{r}, t)$ is a random source of Gaussian noise,

[3] In the cases that $z(\mathbf{r})$ has more than one component, it is necessary to let Γ be a tensor.

uncorrelated in space or in time. In order that Eq. (8) have for its steady state $\exp(-F)$ with F given by Eq. (7), the usual condition

$$\langle \zeta(\mathbf{r}, t)\, \zeta(\mathbf{r}', t') \rangle = 2\Gamma\, \delta(\mathbf{r}-\mathbf{r}')\, \delta(t-t') \tag{9}$$

must be satisfied.

In the context of models of real (rough) interfaces of crystals, Eq. (8) is known as the Edwards–Wilkinson process.[23] There is a large literature on more elaborate equations of this form (usually with nonlinear terms).[24]

To make plausible the assumption of uncorrelated noise, one must consider the action of the microscopic dynamics on the microscopic heights $z(\mathbf{r})$. An elementary dimer flip changes $z(\mathbf{r})$ on just one plaquette by $\pm\Delta z \equiv \pm 4$, and the next dimer flip occurs at another random place. Thus the net height is not conserved, the change is local, and uncorrelated in time, which are modeled by the identical properties of the Langevin noise in (9).

We can Fourier transform the above equations, since periodic boundary conditions maintain translational symmetry. My short-distance cutoff prescription for this continuum field theory shall be that the fields' Fourier transforms have support only in the Brillouin zone $(-\pi, \pi)^2$; in other words, the only allowed $\mathbf{q}$ values are those which are defined for the microscopic lattice model (see Sect. 5). Then (8) becomes

$$\frac{d\tilde{h}_{\mathbf{q}}}{dt} = -\Gamma K\, |\mathbf{q}|^2\, \tilde{h}_{\mathbf{q}} + \tilde{\zeta}_{\mathbf{q}}(t) \tag{10}$$

with Gaussian noise

$$\langle \tilde{\zeta}_{\mathbf{q}}(t)^*\, \tilde{\zeta}'_{\mathbf{q}}(t') \rangle = 2\Gamma\, \delta_{\mathbf{q},\mathbf{q}'}\, \delta(t-t') \tag{11}$$

(Note that $\delta_{\mathbf{q},\mathbf{q}'}$ is the discrete δ-function, appropriate to the discrete lattice of wavevectors corresponding to periodic boundary conditions.) Thus the different Fourier components are decoupled in (10). For each of them (except for $\mathbf{q}=0$), (10) is a one-dimensional Langevin equation with a restoring force.

B. Dynamic Scaling

The correlation function of the heights is easy to derive from the Langevin equation: it is

$$\langle \tilde{h}_{\mathbf{q}}(0)\, \tilde{h}_{-\mathbf{q}}(t) \rangle = \frac{1}{K\, |\mathbf{q}|^2}\, e^{-\lambda_h(\mathbf{q})\, t} \tag{12}$$

where the relaxation rate is

$$\lambda_h(\mathbf{q}) = \Gamma K |\mathbf{q}|^2 \tag{13}$$

Hohenberg and Halperin argued,[16] that the dynamic exponent is best defined by the relation between relaxation rates and wavevectors. Then (13) implies $z = 2$. As a corollary to (13), the smallest relaxation rate of a Fourier mode corresponds to the smallest nonzero wavevector $\mathbf{q}_{\min} = (2\pi/L, 0)$ i.e.,

$$\lambda_h(\mathbf{q}_{\min}) = (4\pi^2 \Gamma K) L^{-2} \tag{14}$$

Random tilings, with vertices not constrained to lie on a periodic lattice, are studied as models of quasicrystals.[17] These too can be mapped to effective interfaces $z(\mathbf{r})$. (A complication, unimportant for the present discussion, is that the height function $z(\mathbf{r})$ or $h(\mathbf{r})$ has two or more components in the quasicrystal cases.) In one case of a quasicrystal random tiling (in three spatial dimensions), (13) was confirmed by simulation.[19] After $z(\mathbf{r}, t)$ was constructed, the data were numerically Fourier transformed to give $\tilde{z}_{\mathbf{q}}(t)$ at selected (small) wavevectors $\mathbf{q}$; for $\mathbf{q}$ small, that is essentially $\tilde{h}_{\mathbf{q}}(t)$. Then the time correlations $\langle \tilde{z}_{\mathbf{q}}(0)\, \tilde{z}_{\mathbf{q}}(t) \rangle$ were fitted to the form (12) and a plot of $\lambda_h(\mathbf{q})$ versus $\mathbf{q}$ revealed the behavior (13). A similar method[7] was used in a study of the Ising antiferromagnet of general spin at $T = 0$ on the triangular lattice, which also has a height representation.

Ref. 18 simulated the random dimer model with dimer-flip dynamics; however rather than periodic boundary conditions, that work used "Aztec diamond" boundary conditions[11] such that $h(\mathbf{r})$ is fixed (and spatially nonconstant) along the edges. The continuum equations below would still predict $\tau(L) \sim L^2$ in that geometry, as was observed in the simulations.[18] Note, though, that they define $\tau(L)$ without the benefit of Fourier analysis, as the mean time it takes two (initially independent) replicas of the system to coincide, when evolved using identical random number sequences.

C. Fokker–Planck Mode Spectrum

Just as the discrete stochastic dynamics implies (1), the continuum stochastic dynamics (8) implies the familiar Fokker–Planck equation for the evolution of the probability density $P(\{\tilde{h}_{\mathbf{q}}(t)\})$,[4]

[4] The customary abuse of notation is committed in which $h_{\mathbf{q}}$ *appears* to be manipulated as if it were a real variable; the convention $dh^*/dh = 0$ justifies the manipulations in (15)–(21).

$$\frac{d}{dt} P(\{\tilde{h}_{\mathbf{q}}(t)\}) = \mathcal{W}_h\{P(\{\tilde{h}_{\mathbf{q}}(t)\})\}$$

$$\Gamma \frac{d}{d\tilde{h}_{\mathbf{q}}} \sum_{\mathbf{q}} \left(\frac{d}{d\tilde{h}_{-\mathbf{q}}} + K\,|\mathbf{q}|^2 \tilde{h}_{\mathbf{q}} \right) P(\{\tilde{h}_{\mathbf{q}}(t)\}) \tag{15}$$

A physicist analyzing the Edwards–Wilkinson dynamics (8) would usually have stopped at (12). That does indeed represent the slowest Fourier mode at each wavevector, but there are many more eigenmodes of the general Eq. (15). These modes are worth computing because (i) they permit computation of more general correlation functions than (12) (ii) the analytic form of the modes, derived below, might inspire improvements on the variational eigenfunctions used in Sect. 5, and (iii) these modes correspond to excited states in the quantum dimer model at its critical point (see Subsect. 1C, above).

The unique zero eigenvalue of Eq. (15), corresponds of course to the Boltzmann distribution which is a Gaussian:

$$P_0(\{\tilde{h}_{\mathbf{q}}(t)\}) \equiv \exp\left(- \sum_{\mathbf{q} \neq 0} \frac{1}{2} K\,|\mathbf{q}|^2 \tilde{h}_{\mathbf{q}} \tilde{h}_{-\mathbf{q}} \right) \tag{16}$$

To construct all the other eigenfunctions, it is convenient to write $\Psi(\{\tilde{h}_{\mathbf{q}}(t)\}) \equiv P(\{\tilde{h}_{\mathbf{q}}(t)\})\, P_0(\{\tilde{h}_{\mathbf{q}}(t)\})^{-1/2}$ so that the time evolution operator of $\Psi(\{\tilde{h}_{\mathbf{q}}(t)\})$ is Hermitian:

$$\frac{d}{dt} \Psi(\{\tilde{h}_{\mathbf{q}}(t)\}) = -\mathcal{H}_h \Psi(\{\tilde{h}_{\mathbf{q}}(t)\}) \tag{17}$$

where

$$\begin{aligned} \mathcal{H}_h &\equiv \Gamma \sum_{\mathbf{q} \neq 0} \left(-\frac{d}{d\tilde{h}_{-\mathbf{q}}} + \frac{1}{2} K\,|\mathbf{q}|^2 \tilde{h}_{\mathbf{q}} \right) \left(\frac{d}{d\tilde{h}_{-\mathbf{q}}} + \frac{1}{2} K\,|\mathbf{q}|^2 \tilde{h}_{\mathbf{q}} \right) \\ &= \sum_{\mathbf{q} \neq 0} \Gamma K\,|\mathbf{q}|^2 \mathscr{C}^{\dagger}_{\mathbf{q}} \mathscr{C}_{\mathbf{q}} \end{aligned} \tag{18}$$

where the "annihilation" operator is

$$\mathscr{C}_{\mathbf{q}} \equiv \left(\frac{1}{2} K\,|\mathbf{q}|^2 \right)^{-1/2} \left(\frac{d}{d\tilde{h}_{-\mathbf{q}}} + \frac{1}{2} K\,|\mathbf{q}|^2 \tilde{h}_{\mathbf{q}} \right) \tag{19}$$

and the corresponding "creation" operator is

$$\mathscr{C}^{\dagger}_{\mathbf{q}} \equiv \left(\frac{1}{2} K |\mathbf{q}|^2\right)^{-1/2} \left(-\frac{d}{d\tilde{h}_{\mathbf{q}}} + \frac{1}{2} K |\mathbf{q}|^2 \tilde{h}_{-\mathbf{q}}\right) \tag{20}$$

Of course $\mathscr{C}^{\dagger}_{\mathbf{q}}$ commutes with $\mathscr{C}_{\mathbf{q}'}$ for all $\mathbf{q}' \neq \mathbf{q}$. Obviously this is mathematically identical to the quantum Hamiltonian for a set of harmonic oscillators with frequencies $\lambda_h(\mathbf{q})$ given by (13), with a "ground state wavefunction" $\Psi_0 = P_0^{1/2}$.

Now we can write any other eigenfunction:

$$\Psi(\{\tilde{h}_{\mathbf{q}}\}; \{n(\mathbf{q})\}) = \left(\prod_{\mathbf{q} \neq 0} (\mathscr{C}^{\dagger}_{\mathbf{q}})^{n(\mathbf{q})}\right) \Psi_0(\{\tilde{h}_{\mathbf{q}}\}) \tag{21}$$

where $\{n(\mathbf{q})\}$ are any nonnegative integers, corresponding to the occupation numbers of the oscillators. When translated back in terms of $P(\{\tilde{h}_{\mathbf{q}}(t)\})$, we see that each eigenstate is a product of $P_0(\{\tilde{h}_{\mathbf{q}}(t)\})$, times polynomials in $\{(\frac{1}{2}K|\mathbf{q}|^2)^{1/2} \tilde{h}_{\mathbf{q}}\}$. For the "elementary excitation" in which $n(\mathbf{q}) = 1$ for one wavevector and zero for all the others, this polynomial is exactly $\tilde{h}_{\mathbf{q}}$; this explains why the correlation function (12) sees only that one eigenmode.

The eigenvalue corresponding to (21) is

$$\lambda_{tot}(\{n(\mathbf{q})\}) = \sum_{\mathbf{q} \neq 0} n(\mathbf{q}) \lambda_h(\mathbf{q}) \tag{22}$$

corresponding to the total energy of the quantum oscillators. The net wavevector is

$$\mathbf{q}_{tot} = \sum_{\mathbf{q} \neq 0} n(\mathbf{q}) \mathbf{q} \tag{23}$$

Notice the many degeneracies resulting from the fact that $\lambda(\mathbf{q}) = \lambda(-\mathbf{q})$: not merely the degeneracies due to global symmetries such as $\mathbf{q} \to -\mathbf{q}$, but less trivial degeneracies such as the one between the mode with $n(\mathbf{q}) = n(-\mathbf{q}) = 1$ and the one with $n(\mathbf{q}) = 2$, $n(-\mathbf{q}) = 0$.

3. HEIGHT-SHIFT MODE

Besides the translations in real space, a height model (as I define it) has the additional symmetry of translations in "height space" (the target space of $z(\mathbf{r})$ and $h(\mathbf{r})$). Correspondingly we will find another kind of slow mode (in a finite system), corresponding to a random walk of the mean height, which I will call the "height-shift mode." It will turn out to be the slowest mode.

Consider the average height

$$\bar{h}(t) \equiv N^{-1} \int_{[0, L]^2} d^2\mathbf{r}\, h(\mathbf{r}, t) \tag{24}$$

i.e., $N^{-1/2}\tilde{h}_0(t)$ (the factor $N^{1/2}$ comes from my normalization convention for Fourier transforms.) Of course, this is just the $\mathbf{q}=0$ mode that was excluded from in the preceding section (e.g., in (21) and (22)). The Langevin equation (8) with $|\mathbf{q}|=0$ tells us $\tilde{h}_0(t)$ simply executes a Gaussian random walk.[5]

When $h(\mathbf{r})$ describes a genuine interface, states with different $\bar{h}$ are all distinct, and the distribution of $\bar{h}$ simply spreads diffusively without ever reaching a steady state. However, in the dimer model (and all other "height models"[1, 5-8]), the height map is one-to-many: here a global shift of $z(\mathbf{r}) \to z(\mathbf{r}) + 4$ describes exactly the same dimer configuration, so the image space of $h(\mathbf{r})$ should be considered a circle of diameter 4. Thus the distribution function, which begins sharply peaked at a particular value of $\bar{h}$, will evolve to a uniform distribution at some rate.

To make this mode more concrete, it may help to compare with the behavior of a spin operator as seen in Appendix A. A system with a height distribution peaked at (say) 1 and 3 has more dimers in one orientation than in the other. As this $n(0)=2$ mode decays, this polarization of orientations will decay; thus these modes have quite real physical meanings.

The random walk behavior (analog of (12)) is

$$\langle |\bar{h}(t) - \bar{h}(0)|^2 \rangle = D(N)\, t \tag{25}$$

with a diffusion constant

$$D(N) = \frac{2\Gamma}{N} \tag{26}$$

It is interesting that although the continuum theory cannot provide the numerical value of the coefficient Γ, it does predict an exact ratio (in the limit $N = L^2 \to \infty$) between the relaxation rate of the modulation $h(\mathbf{q}_{\min}, t)$, and the diffusion rate of the wandering of $\bar{h}(t)$.

[5] This behavior (and the assertions deduced from it) are valid only while the height model is in a "rough" phase. One motivation for understanding the relaxation modes (or quantum energies) is that they might serve as a diagnostic to distinguish rough and smooth phases in simulation results.

A. Fokker–Planck Modes of $\bar{h}(t)$

The Fokker–Planck equation for $\bar{h}$ is simply the diffusion equation; its eigenfunctions are simply plane waves as a function of $\bar{h}$,

$$\psi_Q(\bar{h}) = \exp(iQ\bar{h}) \tag{27}$$

and the corresponding eigenvalue is

$$\lambda_{\bar{h}}(Q) = \tfrac{1}{2}D(N)\, Q^2 \tag{28}$$

with $D(N)$ given by (26). If $\bar{h}$ were diffusing on a line, then any Q would be valid in (28) giving a continuum of eigenvalues.

But, as noted above, a global shift $z(\mathbf{r}) \to z(\mathbf{r}) + 4$ of a microstate corresponds to the same microstate. Thus, the only modes which can correspond to modes in the microscopic model are those periodic under $h(\mathbf{r}) \to h(\mathbf{r}) + 4$; i.e.,

$$Q = n(0)\frac{\pi}{2} \tag{29}$$

for any integer $n(0)$; and the smallest such eigenvalue is

$$\lambda_{\bar{h}}(\pi/2) = \frac{\pi^2 \Gamma}{4N} \tag{30}$$

Thus the *complete* set of eigenfunctions are

$$\Psi(\{\tilde{h}_{\mathbf{q}}\}\,;\,\{n(\mathbf{q}),\, \mathbf{q} \neq 0\})\, \psi_{n(0)\,\pi/2}(\bar{h}) \tag{31}$$

a product of (21) and (27), with any integer $n(0)$. The corresponding eigenvalue is

$$\lambda_{tot}(\{n(\mathbf{q})\},\, \mathbf{q} \neq 0) + n(0)^2\, \lambda_{\bar{h}}(\pi/2) \tag{32}$$

with the first term from (22). The eigenvalue (30) given by $n(0) = \pm 1$ and $n(\mathbf{q}) = 0$ otherwise, is in fact the overall smallest nonzero eigenvalue.[6] Thus (30) is smaller than (14) by a factor $(16K)^{-1}$. From Appendix B, the exact value is $K = \pi/16$ so this ratio is $1/\pi$.

[6] Of course, (30) would not be smallest in the case of $h(\mathbf{r})$ fixed along the boundaries, as in ref. 11 and 20, since that forbids $\bar{h}$-wandering modes. Notice also that, for systems of unequal length sides, the ratio of (14) to (30) is decreased by a factor $L_{\min}/L_{\max}$ so that for a sufficiently elongated system the Fourier mode is the slowest one.

Is the height-shift mode qualitatively distinct from the capillary wave modes? Clearly there is a close connection—the uniform fluctuation of the entire sample of diameter L is much like the fluctuation of one quadrant of a system of diameter $2L$ with a long wavelength Fourier mode. I would argue there *is* a distinction, in that the rate of the $\bar{h}(t)$ relaxation depend on "internal" details of the height model; it cannot be inferred given only the capillary spectrum.

For example, I have noted the fully-frustrated Ising model with single-spin-flip dynamics is identical to the dimer model *except* that it has a height space period of 8 rather than 4. Thus one must replace $\pi/2 \to \pi/4$ in (29) and the smallest eigenvalue (30) is smaller by a factor 1/4. (In the fully-frustrated Ising model, a shift $z \to z+4$ reverses all the spins; thus the mode with $Q = \pm\pi/2$ is the slowest mode that is odd in spin.) In the other direction, I cannot rule out the possibility that in some height model, the stiffness constant K and height periodicity a_h might have numerical values such that $Ka_h^2 > 1$, in which case the slowest mode would be the Fourier mode.

The relationship of the height-shift mode to the capillary wave modes (both of which are a consequence of height-shift sysmmetry), is reminiscent of the relationship between two kinds of low energy excitation in a quantum spin system (both consequences of spin rotational symmetry.) The height-shift mode is the analog of the change in total spin number (giving energies $S(S+1)/2\chi$); the capillary mode is the analog of a spin-wave mode.

4. CORRESPONDENCE TO DISCRETE MODEL

The low-lying modes of the discrete model should be well described by the "quantum numbers" $n(\mathbf{q})$ of the capillary modes and height-shift modes of continuum model.[7] Now, $P_0(\{\tilde{h}_{\mathbf{q}}(t)\})$ corresponds to the eigenmode of the discrete model which has equal weight $p_\alpha^{(0)} = 1/M_0$ for every microstate. Thus the prescription for constructing the approximate eigenmode of the discrete system is

$$p_{\alpha;\, n(\mathbf{q})} \approx \frac{\Psi(\{\tilde{z}_{\mathbf{q}}\};\, \{n(\mathbf{q})\})\, \psi_{n(0)\,\pi/2}(\bar{z})}{\Psi_0(\{\tilde{z}_{\mathbf{q}}\})} \tag{33}$$

[7] The discrete model has additional lattice symmetries (rotations by $\pi/2$ and reflections), which correspond to additional "quantum numbers;" it furthermore has a "locking" tendency (to favor a particular value of $h(\mathbf{r})$ (modulo 1). Discussion of these complications will be deferred to a later publication.[25]

Here $z_{\mathbf{q}}$ is considered an implicit function of the discrete state label α. We obtained (33) simply by replacing $\tilde{h}_{\mathbf{q}} \to z_{\mathbf{q}}$, and $\bar{h} \to \bar{z}$ defined by

$$\bar{z} \equiv N^{-1} \sum_{\mathbf{r}} z(\mathbf{r}, t) \tag{34}$$

which one expects to be valid for small enough $n(\mathbf{q})$ and $\mathbf{q}$.

However, (33) does not map every mode of the continuum equation to an approximate mode of the discrete one. Indeed, since each $n(\mathbf{q})$ is unbounded from above, the continuum kernel $\mathscr{W}_{\tilde{h}}$ has infinitely many independent eigenmodes, whereas the discrete kernel $\mathscr{W}$ has only M_0 eigenmodes. Presumably, when $n(\mathbf{q})$ is so large that $n(\mathbf{q})\,|\mathbf{q}|^2$ is of order unity for some $\mathbf{q}$, the anharmonic terms that I omitted in writing (7) become important and mix this mode with others. Thus only $\mathbf{q}_{tot}$ is a good "quantum number" for labeling the higher modes.

The low-energy eigenstates of the quantum dimer model (5) can be predicted from the above analysis. The wavefunctions should be approximated by (31) and the energies given by (32). These predictions could be compared[25] with the results of recent exact-diagonalization studies on 8×8 lattices.[26]

5. MICROSCOPIC THEORY

Now we return to the exact microscopic dynamics, as introduced in Sect. 1. The microstates are viewed as nodes of a graph in an abstract space, with each possible dimer-flip (and its inverse) forming an edge of the graph: the dynamics described by (1) is a random walk on this graph. As noted already, the graph of microstates with tilt zero has only one connected component. The matrix $\mathscr{W}$ is not only stochastic but symmetric.

A. Variational Bound

The key idea in this section is the use of a variational guess for the eigenfunction. This is mathematically equivalent to the variational bound on the eigenenergy in the quantum dimer model (see Subsect. 1C.)

For any vector $\{\phi_\alpha\}$, the smallest eigenvalue $\lambda_{\min}$ satisfies

$$\lambda_{\min} \leqslant \lambda_\phi \equiv \frac{(\phi^* \mathscr{W} \phi)}{(\phi^* \phi)} \tag{35}$$

Here ϕ^* means the hermitian conjugate. From (2), the numerator is

$$(\phi^* \mathscr{W} \phi) = \sum_{\langle \alpha\beta \rangle} |\phi_\alpha - \phi_\beta|^2 \tag{36}$$

where $\langle \alpha\beta \rangle$ means every pair of microstates, connected by a spin flip, is counted once.

In the two cases considered in this paper (following subsections), $|\phi_\alpha - \phi_\beta| \equiv |\Delta\phi|$ turns out to be the same for every flip move. Then the sum (36) reduces to $\frac{1}{2}|\Delta\phi|^2 \sum_\alpha F_\alpha$ (the 1/2 cancels the double-counting of each graph edge), and finally to $\frac{1}{2} fN |\Delta\phi|^2$. Here f is the probability that a given plaquette is "flippable," i.e., fN is the average "coordination number" of the microstate graph. The exact value[15] is

$$f = 1/8 \tag{37}$$

Meanwhile, the denominator in (35) is just $M_0 \langle |\phi|^2 \rangle$. Thus finally the upper bound is

$$\lambda_\phi = \frac{1}{2} fN \frac{|\Delta\phi|^2}{\langle |\phi|^2 \rangle} \tag{38}$$

When applied to the entire set of eigenvalues of $\mathscr{W}$, Eq. (38) is not very interesting, since we already know that $\lambda_{\min} = 0$ (the eigenvalue of the steady state). However, the variational argument (and every equation in this subsection) is also valid when restricted to a *subspace* orthogonal to that of the ground state. Then, the bound (38) can be useful since the $\lambda_{\min}$ of such a subspace is usually positive.[8] Indeed, the overall smallest nonzero eigenvalue—the goal of this paper (see (4))—is expected to be the $\lambda_{\min}$ of one of these subspaces.

The above variational argument was first presented[27] with a physical interpretation in terms of the normalized dynamic correlation function

$$C_\phi(t) \equiv \frac{\langle \phi(0)^* \phi(t) \rangle}{\langle |\phi|^2 \rangle} \tag{39}$$

Then $C_\phi(t) = 1 - \frac{1}{2}\langle |\phi(0) - \phi(t)|^2 \rangle / \langle |\phi|^2 \rangle$; but at short times, $\langle |\phi(0) - \phi(t)|^2 \rangle \cong \langle |\Delta\phi|^2 \rangle \, fNt$, since there are on average fN independent places where a flip could occur. Thus the upper bound on $\lambda_{\min}$ can be rewritten as the *initial* decay rate of the correlation function,[27]

$$\lambda_\phi = -\left. \frac{dC_\phi(t)}{dt} \right|_{t=0} \tag{40}$$

[8] In subsequent subsections, labels will be attached to $\lambda_{\min}$ to indicate which subspace they belong with, but the labels have been omitted in the general argument here.

Ref. 27 (and similarly ref. 28) applied (40) to bounding the dynamic critical exponent by a function of the static exponents (for a system with nontrivial exponents).

In some circumstances, λ_ϕ could be a good estimate of $\lambda_{\min}$. It would be exact if subsequent steps in ϕ were uncorrelated. (We assume our variational ϕ_α always has nonzero projection onto the slowest mode.) Then $\phi(t)$ performs a random walk, and $C_\phi(t) = \exp(-\lambda_\phi t)$, a pure exponential decay. In light of (3), in which coefficients allowed by symmetry are expected to be generically positive, we would obtain $\lambda_{\min} = \lambda_\phi$.

However, dynamics actually adopted (in Eq. (1) is such that the steps are manifestly anticorrelated in time. For, if a plaquette flips, it must undergo the reverse flip the next time it flips, unless its configuration has been shuffled in the meantime by flips of the adjoining plaquettes. So one would expect (but did not prove!) that $\lambda_{\min} < \lambda_\phi$ as a strict inequality.

B. Fourier Modes

First we review the use of basis states with definite $\mathbf{q}$ vectors. Consider the action of a translation of $\mathbf{r}$; this induces a permutation of microstates which manifestly commutes with $\mathscr{W}$. Thus all eigenvectors must have a definite wavevector $\mathbf{q}$ (or can be chosen thus); that is, a translation by $\mathbf{r}$ simply induces a multiplication by $\exp(i\mathbf{q}\cdot\mathbf{r})$ of the eigenvector. Furthermore $\mathscr{W}$ must have zero matrix elements between vectors with different $\mathbf{q}$; thus $\mathscr{W}$ becomes block-diagonal in the new basis of states with definite $\mathbf{q}$. Hence (35) is valid for the smallest eigenvalue $\lambda_{\min}(\mathbf{q})$ in each block of definite $\mathbf{q}$; that is, if $\{\phi_\alpha\}$ has wavevector $\mathbf{q}$, then

$$\lambda_{\min}(\mathbf{q}) \leqslant \frac{(\phi^* \mathscr{W} \phi)}{(\phi^* \phi)} \tag{41}$$

A suitable variational state-space vector (for $\mathbf{q} \neq 0$) is suggested by the "elementary excitation" eigenfunctions of Subsect. 2C; they consisted of the steady-state eigenfunction Ψ_0 multiplied by $\tilde{h}_q$. The microscopic analog of the gaussian Ψ_0 is the equal-weighted eigenfunction of $\mathscr{W}$, hence we choose

$$\phi_\alpha^{(\mathbf{q})} \equiv \tilde{z}_{\mathbf{q}}(\alpha) \tag{42}$$

(Here $\tilde{z}_{\mathbf{q}}(\alpha)$ means take the configuration $z(\mathbf{r})$ corresponding to microstate α and Fourier transform it for wavevector $\mathbf{q}$).

If α, β are related by one dimer flip on the plaquette at $\mathbf{r}_f$, the corresponding configurations of $z(\mathbf{r})$ differ only by $\pm\Delta z \equiv \pm 4$ at $\mathbf{r}_f$.

Consequently $|\Delta\phi|^2 = |\Delta z|^2/N$. On the other hand, the denominator of (35) is exactly

$$\sum_{\alpha} |\tilde{z}_{\mathbf{q}}(\alpha)|^2 = M_0 \langle |\tilde{z}(\mathbf{q})|^2 \rangle \tag{43}$$

(recall each microstate is weighted equally). Thus the variational bound has the form

$$\lambda_{\min}(\mathbf{q}) \leqslant 8f/\langle |\tilde{z}(\mathbf{q})|^2 \rangle \tag{44}$$

Finally, we know $\langle |\tilde{z}(\mathbf{q})|^2 \rangle \cong 1/K\,|\mathbf{q}|^2$ at small $\mathbf{q}$, as derived in Appendix B. Eq. (B10). This gives the result (for small $\mathbf{q}$)

$$\lambda_{\min}(\mathbf{q}) \leqslant 8fK\,|\mathbf{q}|^2 \tag{45}$$

If we assume (13), then (45) gives a bound on the kinetic coefficient:

$$\Gamma \leqslant \tfrac{1}{2}(\Delta z)^2 f \equiv 8f \tag{46}$$

This approach—constructing a variational vector from the Fourier transform of a local operator—is equivalent to the "single-mode approximation" used for quantum many-body systems such as superfluid helium.[29] Indeed, ref. 21 already noted (in the context of the quantum dimer model) that an exact upper bound on the eigenvalue is implied. Their proposed variational wavefunction is the Fourier transform of an dimer density operator $n_\tau(\mathbf{r})$. In fact, this is actually just $\Delta_\tau z(\mathbf{r})$ (difference operator in the direction $\tau = x, y$); thus their choice differs from (42) only by a derivative. They did not identify the excitations as capillary waves, but derived the exponent $z = 2$ using the correlations of ref. 15.[9]

C. Height-Shift Mode

The variational trick also works for the random walk behavior of (26). Obviously the microscopic analog of (24) is $\bar{z}(t)$ defined by (34). Then the $\mathbf{q} = 0$ modes can be further block-diagonalized into modes with particular wavevectors Q in height space, as defined in Subsect. 3A, hence the variational bound is valid within each such block (to be labeled "$(0; Q)$").

In analogy to (27), we use the variational vector

$$\phi_{\alpha}^{(0;\,Q)} \equiv e^{iQ\bar{z}(\alpha)} \tag{47}$$

[9] Caution: the correlation function exponent entering this calculation is always exactly 2, even when the spin operator exponents decay by exponents $\eta \neq 2$ (see Appendix A). That situation arises in the other height models, or in the dimer model when configurations are weighted unequally.

In this case, $|\Delta\phi| = |\sin(Q\Delta z/2N)|$ for any state α, with $\Delta z = \pm 4$ the same as before, and obviously $|\phi_\alpha| = 1$ in any state. So from (38) we obtain the bound $\lambda_{\min}(0; Q) \leqslant \frac{1}{2} fN \sin^2(4Q/N)$, or

$$\lambda_{\min}(0; Q) \leqslant 8fQ^2/N \tag{48}$$

for large N.

Just like the results (13) and (28) for the two respective kinds of mode in the continuum model, the best variational upper bounds for slow relaxation rates in the microscopic model correspond respectively to $|\mathbf{q}| = |\mathbf{q}_{\min}| = 2\pi/L$ in (45) or to $Q = \pi/2$ in (48). Either kind of bound implies a lower bound on the relaxation time τ which is $O(L^2)$. The better bound comes from (39), and after substituting the value of f (37) gives

$$\tau \geqslant (2/\pi)^2 N \tag{49}$$

It is interesting to note that (48), when compared to (26) and (28), gives the same bound on Γ as Eq. (46) derived from Fourier modes. This might be taken as an approximation for Γ, which amounts (as already noted) to neglecting the anticorrelation of flips. Such an approximation for Γ was made in a random tiling quasicrystal model. (See Sect. 4A and footnote 36 of ref. 19). This turned out[19] to overestimate the true Γ (estimated from the simulation) by about 50%.

6. DISCUSSION

A. Summary

The results in Sect. 2 and 5 exemplify the fruitfulness of Fourier analysis in models with translational symmetry; indeed two types of Fourier transform were used. For capillary wave modes (Sect. 2, and subsect. 5B), the Fourier transform operates with respect to translations in physical space. For height-shift modes (Sect. 3 and Subsect. 5C), it operates on translations in "height space." For each type of mode, two arguments have been given, one based on a coarse-grained field theory (Sect. 2 and 3) and the other based on exact bounds (Sect. 5), which indicate the longest relaxation time scales with system size as L^2.

The only rigorous consequence of the present argument is a *lower* bound (49) on the longest relaxation time. For computational purposes one prefers, of course, an *upper* bound on the time needed to equilibrate the system. Towards this end, the present calculation merely suggests the possible usefulness of Fourier analysis in such a demonstration, and warns

that the slowest mode is not a Fourier modulation at all but the "$\bar{z}$ diffusion" (see Subsect. 3A).

B. Computational Physics

This study is relevant to the dynamics of other spin models. In particular, its results apply directly to the critical dynamics of the fully-frustrated Ising model on the square lattice since that model (at its critical temperature, $T_c = 0$) maps to the dimer covering.[12] The single-spin-flip dynamics in the spin model maps to the dimer-flip dynamics used here.

The derivations could be trivially adapted to the dimer covering of the honeycomb lattice and hence to the critical ($T_c = 0$) dynamics of the triangular Ising antiferromagnet (equivalent to the dimer covering[1]). The behavior argued here can be expected in other spin models which have height representation and single-spin update rules, e.g., the $T = 0$ three-state Potts antiferromagnet on the square lattice (equivalent to the 6-vertex model[31] and hence the BCSOS model). In those cases, however, no exact results or rigorous bounds for the static fluctuations are available to replace Appendix B.

Understanding the local dynamics addressed here is also a prerequisite to addressing the dynamics of height models endowed with loop-update or cluster-update rules, including fully-frustrated Ising models,[32] the three-state Potts antiferromagnet on the square lattice,[33] the BCSOS model,[34] and coloring models.[5][10] More speculatively, it would be interesting to check whether there is any connection between the Swendsen–Wang[35] algorithm and the height representation in the case of the ferromagnetic 4-state Potts model, the partition function of which can be mapped to that of a height model.[36]

Incidentally, the static correlation exponents of height models have been obtained from Monte Carlo simulations much more accurately via Fourier analysis of the heights, than via direct measurement. It seems likely that the same is true for dynamic measurements; this might help in evaluating the dynamic exponent for cluster-acceleration algorithms (see ref. 30).

Somewhat analogous to the loop-update rules are the "zipper moves"[17, 37] of certain random tiling quasicrystal models, such as the (two-dimensional) square-triangle random tiling. In that case, the correlation time was measured to be of $O(1)$ update move per site;[37] however each update move involved $O(L^2)$ sites, so the scaling of the net correlation

[10] It turns out that all the algorithms cited have a simple action on the height variables, thus the existence of a height map may be a prerequisite to the possibility of accelerating such models.

time was $O(N^2)$ just as for the local dimer flip dynamics treated in the present paper.

The height field is the hidden order parameter in the present model (or of height models in general) and hence is the proper way to approach the coarse-grained, long time dynamics. Note that experience has shown that the static exponents are extracted much more efficiently from $\langle |h(\mathbf{q})|^2 \rangle$ than from spin-spin correlations (using the same simulations).[5, 6, 8] Therefore, I suggest numerical studies of the dynamics ought to extract estimates of the correlation times directly from the height fields rather than from spin-spin correlations.

APPENDIX A: CORRELATIONS OF SPIN OPERATORS

This appendix shows that a standard order parameter $m(\mathbf{r})$ of dimer coverings[2, 21] reduces to a function of the heights, and correspondingly its asymptotic correlations are a function of those of the heights. (This works for the standard order parameters of all height models; the derivation for equal-time correlations is discussed at greater length in refs. 1, 5–8.)

Each site $\mathbf{r} = (x, y)$ of the direct (not dual lattice), is connected to one other site $\mathbf{r}' = (x', y')$ by a dimer. Define $m(\mathbf{r}) = (-1)^{x+x'+1}((-1)^{y+y'+1}i)$ for dimers running in the $\pm x(\pm y)$ direction.[11] Then (with the arbitrary constant offset of $z(\mathbf{r})$ fixed as in Fig. 1)

$$m(\mathbf{r}, t) = e^{i(\pi/2)(\bar{h}(\mathbf{r}, t) + 3/2)} \tag{A1}$$

where $\bar{h}(\mathbf{r}, t)$, defined on direct sites, is the average of the four $z(\mathbf{r}, t)$ values on the surrounding dual sites.

Then

$$G(\mathbf{r}, t) \equiv \langle m(0, 0)\, m(\mathbf{r}, t) \rangle \approx \exp\left[-\frac{1}{2}\left(\frac{\pi}{2}\right)^2 C(\mathbf{r}, t) \right] \tag{A2}$$

where

$$C(\mathbf{r}, t) \equiv \langle [\bar{h}(\mathbf{r}, t) - \bar{h}(0, t)]^2 \rangle \tag{A3}$$

Using Fourier transformation with Eqs. (12) and (13), one obtains

$$C(\mathbf{r}, t) = \int \frac{d^2\mathbf{q}}{2\pi} 2[1 - e^{-\Gamma K |\mathbf{q}|^2 t} \cos(\mathbf{q} \cdot \mathbf{r})] \tag{A4}$$

[11] One could equivalently consider $m(\mathbf{r})$ as living on the *occupied bonds*, since $m(\mathbf{r})$ always takes the same value at either end of a dimer.

a logarithmic divergence cut off at high $\mathbf{q}$ by the inverse lattice constant and at small $\mathbf{q}$ by $\min(r^{-1}, [\Gamma Kt]^{-1/2})$. Thus finally the correlation function behaves as

$$G(\mathbf{r}, t) \approx \frac{1}{r^{\eta}_{\pi/2}} \Phi(r/\sqrt{\Gamma Kt}) \tag{A5}$$

where $\Phi()$ is a scaling function, such that $G(r, t) \sim r^{-\eta_{\pi/2}}$ or $G(r, t) \sim (\Gamma Kt)^{-1/2\eta_{\pi/2}}$ depending whether $r/\sqrt{\Gamma Kt}$ is much less than or much greater than unity. This shows that the dynamic critical exponent defined from the standard correlation functions is indeed $z = 2$.[12]

APPENDIX B: STATIC FLUCTUATIONS

This appendix reviews what is known exactly about the equal-time fluctuations of Fourier components of $z(\mathbf{r})$. This result will be an essential lemma for the proof about $\lambda(\mathbf{q})$ outlined in Sect. 5.

Evidently, in the continuum picture, the equal-time expectations are given by

$$\langle \tilde{h}^*_{\mathbf{q}} \tilde{h}_{\mathbf{q}'} \rangle = \delta_{\mathbf{q}, \mathbf{q}'} \frac{1}{K |q|^2} \tag{B1}$$

(Recall that $\tilde{h}^*_{\mathbf{q}} \equiv \tilde{h}_{-\mathbf{q}}$.) This scaling is equivalent to

$$\langle |h(\mathbf{r}) - h(\mathbf{r}')|^2 \rangle = O(1) + \frac{1}{2\pi K} \ln |\mathbf{r} - \mathbf{r}'| \tag{B2}$$

in direct space.

In the study of "height models"[6, 5, 8, 7] and random-tiling quasicrystals,[17] it is the fundamental hypothesis that $\tilde{z}(\mathbf{q})$ has a behavior like (B1) at small $\mathbf{q}$. The behavior (B1) has been proven rigorously for a very limited set of discrete models,[39] and not even for the well-known BCSOS model of rough interfaces.[40] Even though the latter model is "exactly soluble"[41] via the Bethe ansatz, such correlation functions are not known exactly (correlation functions are notoriously difficult to extract from the Bethe ansatz method[42]).

However, the dimer covering model (with 2D Ising models) belongs to the "free-fermion" class of exactly soluble models,[9, 10] and using the

[12] Eq. A5 was previously derived in the context of the hexatic order parameter: see Eq. (5.13) of ref. 38.

Pfaffian approach the dimer-dimer correlation functions can (in principle) be written out exactly.[15] Later on McCoy evaluated the large-distance asymptotic behavior of the correlation function, for any orientation of the vector between the two dimers.[43]

Say that $n_x(\mathbf{r}) = 1$ when there is a dimer connecting $\mathbf{r}$ to $\mathbf{r} + [1, 0]$ and zero otherwise; $\delta n_x(\mathbf{r}) \equiv n_x(\mathbf{r}) - \langle n_x(\mathbf{r}) \rangle \equiv n_x(\mathbf{r}) - \frac{1}{4}$, similarly for $n_y(\mathbf{r})$.

It was computed[15] that, in the equal-weighted ensemble of dimer coverings,

$$C_{xx}(\mathbf{R}) \equiv \langle \delta n_x(\mathbf{r})\, \delta n_x(\mathbf{r}') \rangle = -g(X, Y)^2 + g(X+1, Y)\, g(X-1, Y) \tag{B3}$$

Here $\mathbf{R} \equiv (X, Y) \equiv \mathbf{r}' - \mathbf{r}$, and $g(X, Y)$ is a Green's function arising from the Pfaffians.[15] At large $\mathbf{R}$,

$$g(X, Y) \cong \begin{cases} -\dfrac{1}{\pi}\dfrac{Y}{R^2}, & X \text{ odd, } Y \text{ even;} \\ \dfrac{i}{\pi}\dfrac{X}{R^2}, & X \text{ even, } Y \text{ odd;} \\ 0 & \text{otherwise} \end{cases} \tag{B4}$$

Hence, collecting the four cases (X and Y even or odd),

$$C_{xx}(X, Y) \cong \frac{1}{2\pi^2}\left[(-1)^{X+Y}\frac{Y^2 - X^2}{R^4} + (-1)^X \frac{1}{R^2} \right] \tag{B5}$$

Dimer correlations imply correlations in height gradients since the definition of $z(\mathbf{r})$ (Sect. 1) is equivalent to

$$z(\mathbf{r} + [\tfrac{1}{2}, \tfrac{1}{2}]) - z(\mathbf{r} + [-\tfrac{1}{2}, \tfrac{1}{2}]) = (-1)^{x+y} 4\delta n_y(\mathbf{r}) \tag{B6a}$$

$$z(\mathbf{r} + [\tfrac{1}{2}, \tfrac{1}{2}]) - z(\mathbf{r} + [\tfrac{1}{2}, -\tfrac{1}{2}]) = (-1)^{x+y+1} 4\delta n_x(\mathbf{r}) \tag{B6b}$$

Combining (B5) and (B6b), with

$$z(\mathbf{r} + [\tfrac{1}{2}, \tfrac{1}{2}]) - z(\mathbf{r} + [\tfrac{1}{2}, -\tfrac{1}{2}]) \to \nabla_y z(\mathbf{r}) \tag{B7}$$

gives

$$\langle \nabla_y z(\mathbf{r})\, \nabla_{y'} z(\mathbf{r}') \rangle \cong \frac{4^2}{2\pi^2}\left[\frac{Y^2 - X^2}{R^4} + (-1)^Y \frac{1}{R^2} \right] \tag{B8a}$$

The term in (B8a) multiplied by $(-1)^Y$ will be neglected since it averages to zero. Similarly, using the analogous formulas for $\langle \delta n_x \, \delta n_y \rangle$,

$$\langle \nabla_x z(\mathbf{r}) \, \nabla_{y'} z(\mathbf{r}') \rangle \cong -\frac{4^2}{2\pi^2} \frac{2XY}{R^4} \tag{B8b}$$

and

$$\langle \nabla_x z(\mathbf{r}) \, \nabla_{x'} z(\mathbf{r}') \rangle \cong -\frac{4^2}{2\pi^2} \left[\frac{X^2 - Y^2}{R^4} + (-1)^X \frac{1}{R^2} \right] \tag{B8c}$$

The non-oscillating correlations in Eqs. (B8) have the form of dipole-dipole interactions, as if $\nabla z(\mathbf{r})$ is a polarization.[43] Integrating these equations with respect to $\mathbf{R}$,

$$\langle |z(\mathbf{r}) - z(\mathbf{r}')|^2 \rangle \cong \text{const} + \frac{16}{\pi^2} \ln |\mathbf{r} - \mathbf{r}'| \tag{B9}$$

and Fourier transforming yields the required result,

$$\langle |\tilde{z}(\mathbf{q})|^2 \rangle \cong \frac{16}{\pi |\mathbf{q}|^2} \tag{B10}$$

The behavior is indeed described by the continuum mode (B1), with $K = \pi/16$.

An exact result for arrow-arrow correlations was also obtained for a special case of the 6-vertex model,[14] and applied to compute exactly the coefficient of the logarithmic asymptotic behavior of $\langle |z(\mathbf{r}) - z(\mathbf{r}')|^2 \rangle$ for the corresponding BCSOS model.[44] (The BCSOS model is just the height mapping of the 6-vertex model). Actually, the parameter values in that special case make it equivalent to a random dimer covering. To convert the $h(\mathbf{r})$ of the dimer model to the height $h_{BCSOS}(\mathbf{r})$ of a BCSOS model (with lattice constant $\sqrt{2}$), put $h(\mathbf{r})/2 = h_{BCSOS}$ on the sublattice with even $h(\mathbf{r})$ and erase $h(\mathbf{r})$ on the sublattice where it is odd. (See also ref. 45; to relate this to other versions of the same mapping between models[46] reverse all the arrows pointing along vertical bonds).

ACKNOWLEDGMENTS

I am grateful to D. Randall, and P. W. Leung for stimulating discussions, and to C. Zeng, J. Kondev, and J. Propp for helpful comments on the manuscript. I thank the Institute for Advanced Study for hospitality. This work was supported by NSF grant DMR-9612304.

REFERENCES

1. H. W. J. Blöte and H. J. Hilhorst, *J. Phys. A* **15**:L631 (1982); B. Nienhuis, H. J. Hilhorst, and H. W. J. Blöte, *J. Phys. A* **17**:3559 (1984).
2. W. Zheng and S. Sachdev, *Phys. Rev. B* **40**:2704 (1989).
3. L. S. Levitov, *Phys. Rev. Lett.* **64**:92 (1990).
4. W. Thurston, *Amer. Mathematical Monthly* **97**:757 (1990).
5. J. Kondev and C. L. Henley, *Phys. Rev. B* **52**:6628 (1995).
6. R. Raghavan, C. L. Henley, and S. L. Arouh, *J. Stat. Phys.* **86**:517 (1997).
7. C. Zeng and C. L. Henley, *Phys. Rev. B* **55**:14935 (1997).
8. J. K. Burton and C. L. Henley, "Constrained antiferromagnetic Potts model with an interface representation" submitted to *J. Phys. A*.
9. M. E. Fisher, *Phys. Rev.* **124**:1664 (1961).
10. P. W. Kasteleyn, *Physica* **27**:1209 (1961).
11. H. Cohn, N. Elkies, and J. Propp, *Duke Math. J.* **85**:117 (1996).
12. J. Villain, *J. Phys.* **C10**:1717 (1977).
13. E. H. Lieb, *J. Math. Phys.* **8**:2339 (1967).
14. B. Sutherland, *Phys. Lett.* **26A**:532 (1968).
15. M. E. Fisher and J. Stephenson, *Phys. Rev.* **132**:1411 (1963).
16. P. C. Hohenberg and B. I. Halperin, *Rev. Mod. Phys.* **49**:435 (1977).
17. C. L. Henley, in *Quasicrystals: The State of the Art*, ed. P. J. Steinhardt and D. P. DiVincenzo (World Scientific, 1991).
18. J. Propp, unpublished.
19. L. J. Shaw, V. Elser, and C. L. Henley, *Phys. Rev. B* **43**:3423 (1991).
20. M. Luby, D. Randall, and A. Sinclair, in *Proc. 36th Annual Symposium on Foundations of Computer Science* (IEEE Computer Science Press, Los Alamitos CA, USA, 1995).
21. D. S. Rokhsar and S. A. Kivelson, *Phys. Rev. Lett.* **61**:2376 (1988).
22. P. M. Chaikin and T. C. Lubensky, *Principles of Condensed Matter Physics* (Cambridge University Press, 1995).
23. S. F. Edwards and D. L. Wilkinson, *P. Roy. Soc. Lond. A* **381**:17 (1981).
24. A.-L. Barabasi and H. E. Stanley, *Fractal Concepts in Surface Growth* (Cambridge University Press, 1995).
25. C. L. Henley, unpublished.
26. P. W. Leung, K. C. Chiu, and K. Runge, *Phys. Rev. B* **54**:12938 (1996).
27. B. I. Halperin, *Phys. Rev. B* **8**:4437 (1973).
28. X.-J. Li and A. D. Sokal, *Phys. Rev. Lett.* **63**:827 (1989).
29. R. P. Feynman, in *Progress in Low-Temperature Physics*, vol. 1, ed. C. Gorter (North-Holland, 1955).
30. P. D. Coddington and L. Han, *Phys. Rev. B* **50**:3058 (1994).
31. E. H. Lieb and F. Y. Wu, in *Phase Transitions and Critical Phenomena* v. I, ed. C. Domb and M. S. Green. (Academic Press, 1972).
32. D. Kandel, R. Ben-av, and E. Domany, *Phys. Rev. Lett.* **65**:941 (1990); D. Kandel and E. Domany, *Phys. Rev. B* **43**:8539 (1991).
33. J-S. Wang, R. H. Swendsen, and R. Kotecký, *Phys. Rev. Lett.* **63**:109 (1989); *Phys. Rev. B* **42**:2465 (1990).
34. H. G. Evertz, G. Lana, and M. Marcu, *Phys. Rev. Lett.* **70**:875 (1993).
35. R. H. Swendsen and J-S. Wang, *Phys. Rev. Lett.* **58**:86 (1987).
36. B. Nienhuis, in *Phase Transitions and Critical Phenomena*, edited by C. Domb and J. L. Lebowitz (Academic, London, 1987), Vol. 11.
37. M. Oxborrow and C. L. Henley, *Phys. Rev. B* **48**:6966 (1993).

38. D. R. Nelson, in C. Domb and J. L. Lebowitz, *Phase Transitions and Critical Phenomena*, Vol. 7 (Academic Press, 1983).
39. J. Fröhlich and T. Spencer, *Phys. Rev. Lett.* **46**:1006 (1981); *Commun. Math. Phys.* **81**:527 (1981).
40. T. Spencer, private communication (1996).
41. H. van Beijeren, *Phys. Rev. Lett.* **38**:993 (1977).
42. R. J. Baxter, *Exactly Solved Models in Statistical Mechanics* (Academic Press, 1982).
43. R. W. Youngblood, J. D. Axe, and B. M. McCoy *Phys. Rev. B* **21**:5212 (1980). (see their Appendix A.)
44. D. B. Abraham, in C. Domb and J. L. Lebowitz, *Phase Transitions and Critical Phenomena*, Vol. 10 (Academic Press, 1986); see his Sect. 7B.
45. R. J. Baxter, *Ann. Phys.* (N.Y.) **70**:193 (1972). (See his Appendix A).
46. B. Sutherland, unpublished.